PAPER

Chemical characterization of automobile windshield glass samples for major, minor, and trace elemental concentration determination by INAA and its comparison with ED-XRF and DC Arc AES in terms of analytical capabilities and possible applications for glass forensics

Vishal Sharma, [ID] [ab] Arijit Sengupta, [ID] *[bc] Raghunath Acharya [ID] *[bc] and Hemlata K. Bagla[a]

Automobile (car) windshield glass fragments serve as important forensic evidentiary materials and their chemical characterization mainly at minor and trace concentration levels is a key step in forensic investigations. For such glass analysis as well as for forensics, direct solid sample analysis by suitable analytical technique(s) is very important. In view of this, instrumental neutron activation analysis (INAA) using high flux neutrons from research reactor was utilized for chemical characterization of car windshield glass samples. Energy dispersive X-ray fluorescence (ED-XRF) and direct current arc carrier distillation atomic emission spectroscopy (DC Arc AES) methods were also utilized for the analysis of all glass samples for evaluating their analytical capabilities with respect to INAA. A comparative evaluation was carried out with respect to accuracy, precision, and detection limits under quality assurance/quality control (QA/QC). The methods were validated by analyzing certified reference materials (CRMs) G-2 and RGM-1 from USGS and NIST standard reference material (SRM) of sodalime glass (SRM 610). Concentrations of seventeen elements (Na, Ca, Sc, Cr, Fe, Co, Zn, Rb, Zr, Ba, La, Hf, Ce, Eu, Yb, Sm, and Th) were determined in all analyzed glass samples by INAA at major, minor, and trace concentration levels, indicating its capability for potential applications to forensic studies. Grouping study of these automobile glasses was carried out utilizing concentrations of transition elements and rare earth elements (REEs) in conjunction with statistical cluster analysis. In addition, it has been highlighted that some of the transition elements as well as REEs are important markers/discriminating elements for same brand automobile glasses obtained from two different sources/origins.

[a]*Department of Nuclear and Radiochemistry, Kishinchand Chellaram College, Mumbai 400020, India*

[b]*Radiochemistry Division, Bhabha Atomic Research Centre, Mumbai 400085, India. E-mail: racharya@barc.gov.in; arijita@barc.gov.in*

[c]*Homi Bhabha National Institute, Anushaktinagar, Mumbai 400094, India*

1. Introduction

Glasses have become the important ingredient of the modern society. It has diverse applications toward indoor and outdoor purposes including container glass, utensils, laboratory glassware, nuclear waste storage, automobile windshield glass, energy (photovoltaic), science exploration communication, architecture, and decoration.[1,2] Compositional characterization of a glass sample is useful to ascertain its physical and chemical properties. For example, the immobilization capacity of high-level liquid waste into borosilicate glass matrix is generally increased by adding elements such as P, Fe, Ba, and Pb.[3–5] The minor and trace elemental concentrations including rare earth elements (REEs) of glassy materials are also important diagnostic tools for archeological and forensic analyses to find out the source/origin of glasses.[6–8] Statistical approaches, namely, likelihood ratio, Naïve Bayes classifiers, and support vector machine were utilized for the classification of glasses for potential forensic applications.[9,10] Multivariate model involving empirical cross entropy (ECE) function was calibrated for discriminating the glass samples.[11] In view of the importance of automotive glasses as a forensic evidence, a comprehensive study by determining elemental concentrations has been undertaken in the present investigation.

Automobile window/windshield glasses are basically soda-lime glasses with Si, Na, Ca, Mg, and Al as major elements along with minor and trace elements, including transition metals and REEs. These glasses are often investigated as

forensic evidences in hit and run cases, accident, and vandalism by forensic scientists due to their inertness and chemical stability with respect to weathering and long-term storage. Such objects are examined by qualitative/quantitative means to ascertain their chemical composition and possible sources/origin, the prime focus of forensic investigation.[8] Comprehensive analysis of solid samples having complex matrices (as in the case of glass) is very difficult with conventional analytical techniques such as atomic absorption spectrometry (AAS),[12] electron probe microanalysis (EPMA),[13] scanning electron microscopy energy dispersive X-ray (SEM-EDX),[14,15] inductively coupled plasma optical emission spectroscopy (ICP-OES), and inductively coupled plasma mass spectrometry (ICP-MS).[16–19] These techniques sometimes require cumbersome procedure for sample digestion, reagent blank, and laborious matrix separation methods. These techniques, in conjunction with lasers are useful for the direct sample analysis.[20–28] Radio-analytical techniques such as energy dispersive X-ray fluorescence (ED-XRF)[29] and accelerator/reactor-based techniques, namely, particle induced gamma-ray emission (PIGE), particle induced X-ray emission (PIXE), and instrumental neutron activation analysis (INAA) are utilized for the analysis of glass samples due to their nondestructive nature and capability of simultaneous multi-elemental determination.[8,29–32] These methods are advantageous over conventional spectroscopic methods in terms of reagent blank correction, non-destructive in nature, no matrix separation, and minimum sample handling.

Various analytical techniques that have been utilized for chemical characterization of glasses toward potential forensic applications are laser ablation inductively coupled plasma mass spectrometry (LA-ICP-MS),[22,23,33–36] X-ray fluorescence spectroscopy,[37] a combination of μ-XRF, SN-ICP-MS, LA-ICP-MS, and LA-ICP-OES,[38] a comparison of (LA-ICP-MS) and ICP-MS,[21] comparison of μ-XRF, ICP-MS, and LA-ICP-MS;[39] and micro X-ray fluorescence spectrometry.[40] Comprehensive reviews and other literature are also available in recent years.[35,41–44] This revealed that the elemental characterization of glass matrix is of high importance and high relevance even in today's scenario. Moreover, none of the reports were seen in the literature since early 90s, where NAA was used for elemental characterization of glass with potential importance to forensics. In view of this, the present work deals with the analyses of glass samples by INAA to revisit its capabilities as well as its QA/QC for automobile glass samples. Corzo *et al.* [2021] have used the combination of micro-XRF and refractive index measurement for the interpretation of glass evidences for forensic applications.[44] Our laboratory has no facility for the measurement of the refractive index of the glass samples. Thus, our group has decided to choose multiple analytical techniques having different working principles, which includes one of the reference techniques, *i.e.*, NAA, which has been extensively applied in diverse fields. The analytical capabilities of the INAA method were compared with the DC Arc AES and ED-XRF methods. All three methods are capable of analyzing the solid sample, *i.e.*, there is no need of dissolution of sample or minimum sample preparation steps are involved which reduces the chance of contamination and

error in the analyses. Elemental concentration results obtained from these methods were compared and independently utilized for the grouping study using the cluster analysis approach for possible forensic applications. Though ICP-OES has been used, however, the dissolution of such glass matrix to form the solution is highly cumbersome. There is also a chance of cross contamination as well as element loss during the processing of glass samples.

ED-XRF is a semi-quantitative, fast, and non-destructive technique capable of analyzing solid samples either directly or in the pellet form for major and minor analytes.[45–47] It has also been exploited for the compositional analysis of forensically important glass samples.[17] Direct Current Arc carrier distillation Atomic Emission Spectrometry (DC Arc AES) is one of the multi-elemental techniques routinely used for chemical quality control (CQC) of different materials including nuclear materials, refractory powders, glass, ceramics, and precious metals[48–50] for minor, trace, and even ultratrace level. However, poor precision (RSD $\sim$ 9–15%) and inability of trace level determination of REEs are some of the intrinsic drawbacks.[48–50] INAA is a nuclear analytical technique capable of determining many elements spanning from Na to U at major, minor, and trace concentration levels simultaneously for various materials, including biological, geological, environmental, nuclear materials, glass, ceramic/refractory-based finished products, and forensic samples.[51] The advantageous properties of INAA are isotope specific, nondestructive, multi-elemental in nature, direct (as received) solid sample analysis, minimum sample handling, requirement of small sample size (1–100 mg), inherent accuracy and precision, and sensitivity due to high flux neutron (10^{11}–10^{14} n cm^{-2} s^{-1}) from research reactors for activation. The lower mass (1–10 mg), though not advisable and not representative in routine analysis, is used in special cases when the sample mass available is very low or when high neutron flux is used. This method is very sensitive to many trace elements including REEs and is able to quantify down to the ppb concentration level with adequate accuracy and precision.

In the present work, a comprehensive investigation was carried out for the chemical characterization of automobile windshield glasses exploiting ED-XRF, DC Arc AES, and INAA. These three different analytical techniques have been optimized for the quantification of major to trace elements in car windshield glasses (sodalime glasses) and their capabilities have been compared in terms number of elements determined, validation or accuracy of the method, precision (uncertainty), and detection limits. Methods have been validated using geological as well as glass certified reference materials. Interday fluctuation/variation in the results has also been evaluated for XRF- and AES-based methods. The effect of lower size of the sample (*i.e.*, 2 mg) was also studied with DC Arc AES and INAA methods. Grouping studies were carried out utilizing elemental concentrations and their ratios obtained by all the three methods in conjunction with statistical cluster analysis. The potential of INAA has been highlighted for forensic applications by means of grouping study utilizing minor and trace elemental

concentrations including transition and rare earth elements (REEs).

2. Experimental

2.1 Materials

Six different automobile/windshield glasses (GA to GF) were collected from the local motor market as per American Standard Test Method (ASTM) regulations for glass samples.[52,53] AgCl used in the present study was procured from SPEX Industries (Metuchen, NJ, USA). Multielemental standards of spec pure grade solutions procured from E-Merck, Germany, were used in the present case. Method validation was carried out by analyzing three geological certified reference materials (CRMs), namely, USGS G-2 (granite), USGS STM-1 (syenite), and USGS RGM-1 (rhyolite), which were purchased from United States Geological Survey (USGS) and one sodalime glass reference material NIST SRM 610, which was purchased from NIST, USA. Out of these, USGS STM-1 was considered as the standard reference material and the other three, namely, USGS G-2, RGM-1, and NIST SRM 610 were used as the control samples; the corresponding results are tabulated later in the method validation section. In addition, INAA has been applied to two automobile glasses of foreign (Israel) origin for comparison with similar brand glasses of local (Indian) origin.

2.2 Instrumentation

ED-XRF experiment was carried out using Jordan Valley EX3600M spectrometer with stabilized X-ray tube and Rh as X-ray source. 150 mg powder glass sample was used for X-ray irradiation in air atmosphere and ambient temperature. The emitted X-ray photons were measured using Si(Li) detector coupled with a multichannel analyzer (MCA). The resolution achieved through this instrument was found to be 0.139 keV at Mn-Kα (5.9 keV). The typical schematic for ED-XRF analysis is shown in Fig. 1. The optimized instrumental and experimental parameters for the ED-XRF analysis of automobile glasses are summarized in Table 1.

The direct solid sample was analyzed utilizing DC Arc carrier distillation technique with an atomic emission spectrometer, Spectro-Arcos, Germany. The instrumental parameters were
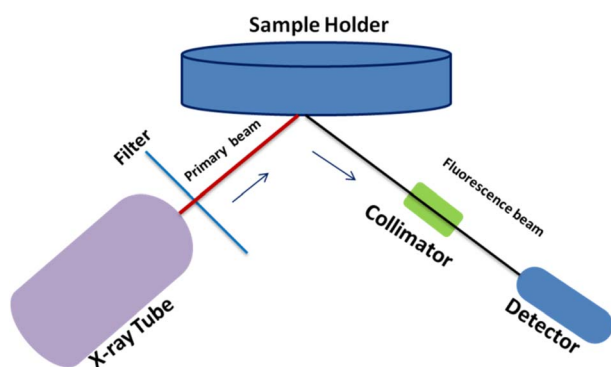

Fig. 1 Typical schematic for ED-XRF analysis.

Table 1 Optimized instrumental parameters for ED-XRF analysis of the glass samples

Parameters	Value
Target	Rh
Filter	No filter
High voltage	30 kV
Emission current	200 μA
Preset time	200 s
Atmosphere	Air
Energy range	40 keV

Table 2 Optimized experimental parameters for the DC Arc AES method for glass analysis

Instrumental specification	
Optical design	Paschen–Runge mounting
Grating	Holographic
Groove density	1800 grooves per mm
Total wave length range	130–800 nm
Resolution (FWHM)	0.01 nm from 130–450 nm
	0.02 nm from 450–800 nm
Thermal isolation	Controlled to 30 $\pm$ 1 °C
Detector	Charge couple device (CCD)
Detector arrangement	Linear arrays of 3648 pixels per array

optimized and are summarized in Table 2. A standard carrier distillation type electrode, ASTM designation E-130-66 type S-2 (cup shaped electrode), lower electrode, was used as the anode, whereas the pointed electrode (upper one), ASTM designation E-130-66 type C-1, was used as the cathode.[48–50]

For instrumental neutron activation analysis (INAA), direct solid powdered samples ($\sim$50 mg) were irradiated using high flux ($\sim$10^{13} n cm^{-2} s^{-1}) reactor neutrons for 6 h in self-serve facility of Dhruva research reactor, BARC, India. Radioactive assay was carried out using high purity germanium (HPGe) detector with 50% relative efficiency. The resolution achieved was found to be 1.9 keV at 1332 keV of ^{60}Co. The experimental procedure involving various steps from sample preparation to radioactive assay for the INAA method is summarized in Fig. 3. Gamma ray measurement was carried out using PC-based MCA having 4k channel. The peak area analyses for both the sample and standard were carried out using Peak Height Analysis Software (PHAST) developed by BARC through low exponential tail model for peak fitting.[8,54]

2.3 Methods

For ED-XRF, the sample and standards were irradiated using X-ray (emission current = 200 μA) from the Rh source with a maximum energy of 40 keV for 200 s. The emitted X-rays from the target were measured using the Si(Li) detector. Peak area selection for both the sample and standard was carried out using in-built software. For DC Arc AES, a charge was prepared by mixing 45–50 mg of sample with 5% AgCl. AgCl was used as a carrier to sweep away the minor and trace analytes from the glass matrix as their respective chlorides, keeping emission
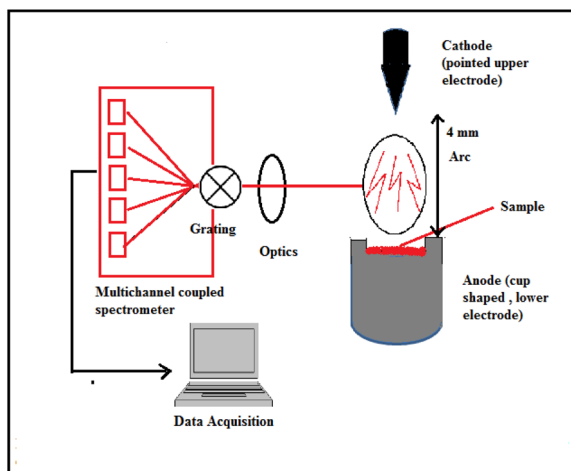
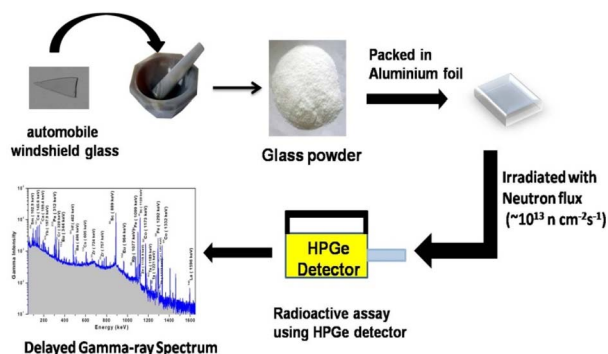Fig. 2 Sample introduction in the DC Arc carrier distillation AES technique.

Fig. 4 Gamma ray spectrum of neutron-irradiated automobile glass using the self-serve facility of Dhruva research reactor, BARC, Mumbai.

Fig. 3 Experimental procedure for the INAA method.

For INAA, the samples and standard were packed in ultra-pure aluminium foil separately and co-irradiated with neutron flux of $\sim 10^{13}$ n cm^{-2} s^{-1}. The irradiated samples/standards were repacked in fresh (i.e., inactive) aluminium foil after appropriate cooling time and reweighed to take the actual weight of the sample. Subsequently, samples and standards were mounted on Perspex plates separately to maintain the similar geometrical conditions of samples and standard with respect to the detector. Radioactive assay was carried by short, medium, and long counting time, i.e., 10 min, 4–5 h, and 12–14 h, respectively.[8,51,54] The typical gamma-ray spectrum of a neutron-irradiated automobile glass using the self-serve facility of Dhruva research reactor at BARC is shown in Fig. 4.

2.4 Concentration calculation

The absolute elemental concentration for ED-XRF and DC Arc AES methods was calculated by considering the counts under the photo peak by relative methods. For INAA, the absolute concentration values were calculated by comparing the decay corrected count rates of the sample with the standard reference materials using the relative method of INAA.[8,51,54]

$$m_{\text{x,sample}} = m_{\text{x,std}} \times \frac{\text{cps}_{\text{x,sam}}}{\text{cps}_{\text{x,std}}} \times \frac{D_{\text{std}}}{D_{\text{sample}}} \qquad (1)$$

where '$m_{\text{x,sample}}$' is the mass of analyte of interest in the samples, $m_{\text{x,std}}$ is the mass of analyte in the standard, cps is the count rate of gamma-ray of interest, and 'D' is decay factor ($e^{-\lambda t}$), where 'λ' is decay constant and 't' is cooling time between end of irradiation and start of measurement.

3. Results and discussion

The chemical characterization of forensically important glass samples, i.e., automobile windshield glasses was carried out using a combination of three different radio-analytical and nuclear analytical techniques.

rich matrix elements into the electrode in the form of refractory oxides. The resulting charge was introduced inside the anode (graphite) and tapped from above to ensure proper packing, while venting was made inside the anode as an outlet for the gases generated during arcing. An arc with temperature ~ 3000 °C at the analytical zone was used as the excitation source, while the charged coupled device (CCD) was used as the detector system.[48–50] During the ignition of the arc, the electrons from the cathode were discharged and struck on the samples in the cup-type anode. Resistive heating is responsible for the excitation and subsequent emission. Suitable, interference-free analytical lines of each analytes were identified and used for their determination. The detailed carrier distillation technique was published elsewhere.[48–50] The standards for trace elements were prepared by homogeneously grinding the synthetic glass (with known concentrations of major elements, namely, Si, Na, Mg, and Al) with known amount of multi-elemental spectroscopy grade pure solution. Similar sets of standards were used for ED-XRF. The arrangement of sample introduction in the DC Arc AES assembly is shown in Fig. 2.
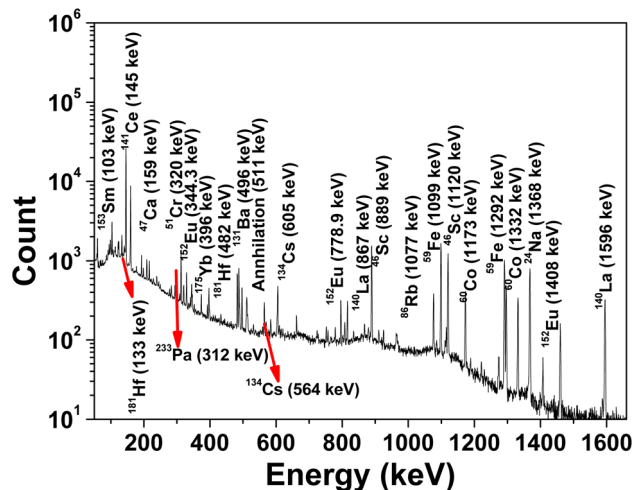
3.1 Quality assurance and quality control (QA/QC) of analytical techniques

QA/QC in measurements have been discussed here, where the following analytical parameters have been evaluated and discussed under QA such as detection limits, uncertainty measurement/precision, and method validation (QC), and the obtained results are discussed briefly.

3.1.1 Evaluation of analytical performances: sensitivity and limit of detection (L_D).

The limit of detection (L_D) ($\mu g\ g^{-1}$ or ppm) for ED-XRF and DC Arc AES methods was calculated by taking the analyte solutions with varying concentrations. The slope of the calibration plot, i.e., count rate vs. concentration of analyte was used as the sensitivity (cps per ppm) and the L_D values for ED-XRF and DC Arc AES methods were calculated using eqn (2) given below.

$$L_D = 3a^{-1}(\text{Blk})^{1/2} \qquad (2)$$

where 'a' is the slope of the calibration curve and 'Blk' is the blank peak area.

For INAA, L_D (in ppm) was calculated from eqn (3) and is given below.

$$L_D = \frac{\dfrac{3 \times (\text{Bkg})^{1/2}}{\text{LT} \times S\ (\text{cps per } \mu g)}}{W\ (g)} \qquad (3)$$

where 'Bkg' is the background counts (peak area) given by eqn (3), 'LT' is the live time of counting or radioactive assay, 'S' is the sensitivity (cps per μg), and 'W' is the sample mass taken for the analysis in 'g'. The background counts (Bkg) under the photo peak of the analyte of interest were calculated from the sample spectrum by taking the difference in the gross and net counts given by eqn (4).

$$\text{Bkg} = \text{gross counts} - \text{net counts} \qquad (4)$$

The sensitivity (cps per μg) used for the L_D calculation was calculated from the certified elemental concentrations of USGS CRM STM-1 (syenite) and expressed by eqn (5).

$$S_x = \frac{\text{CPS}_x(\text{count rate})}{m_x(\text{mass})} \qquad (5)$$

where 'S_x' is the sensitivity of the analyte 'x', 'CPS' is the count rate of the analyte, and 'm_x' is the mass (μg) certified to be present in the reference material.

The obtained experimental values of L_D (ppm or $\mu g\ g^{-1}$) for ED-XRF, DC Arc AES, and INAA in the present work along with the literature values for all the three methods are given in Table 3. The estimated L_D values for different analytes by the ED-XRF and DC Arc AES methods were found to vary in the range of 25 to 62 ppm and 5 to 90 ppm, respectively. For INAA, the L_D value was found to vary from 20 ppb to 140 ppm for Na_2O, Sc, Cr, Fe_2O_3, Co, Zn, Rb, Zr, Ba, Hf, and Th, while for REEs, the detection limits were found to be very low (Sc, La, Ce, Eu, Yb, and Sm), i.e., varying from 20 ppb to 0.7 ppm. In DC Arc AES-based carrier distillation technique, the analytes, which have the tendency to form refractory oxides such as REEs have shown poorer L_D values. The experimentally obtained L_D values in the present work were found to be comparable to the literature values for almost all the elements of interest.

Table 3 Comparison of experimental and literature values of limit of detection (L_D) values by ED-XRF, DC Arc AES, and INAA methods[a]

| Element/oxide | Limit of detection (L_D) values (mg kg^{-1} or ppm) | | | | | |
| | ED-XRF | | DC Arc AES | | INAA | |
	This work	Literature[49,50,55–57]	This work	Literature[49,50,55–57]	This work	Literature[51]
SiO$_2$	62	40–100	35	80	ND	ND
Na$_2$O	30	10–30	10	2–5	6	2–10
CaO	25	15–45	15	5	50	700–4000
Sc	35	NA	5	NA	0.02	0.001–0.02
Cr	28	20–40	5	5	0.65	1
Fe$_2$O$_3$	25	50	8	10	140	8–100
Co	30	20	4	5	0.1	0.02–0.3
Zn	27	20–40	7	5–10	2.2	0.4–6
Rb	ND	NA	ND	NA	1.5	0.4–6
Zr	36	45	90	NA	22	5–80
Ba	40	50	10	10	1.3	10–40
La	25	NA	75	NA	0.08	0.1–0.3
Hf	ND	NA	ND	NA	0.05	0.01–0.1
Ce	25	NA	80	NA	0.7	0.2–1
Eu	30	30	60	80	0.05	0.006–0.05
Yb	27	NA	90	NA	0.08	0.03–0.2
Sm	35	NA	68	NA	0.02	0.01–0.03
Th	NA	NA	NA	NA	0.1	0.01–0.1
Sr	30	NA	10	NA	ND	5–60

[a] ND – not detected and NA – not available.

3.1.2 Evaluation of uncertainties from relative standard deviation.

The uncertainties associated with each method is expressed by the calculation of the unweighted standard deviation at ± 1 s confidence limit (eqn (6)) and calculation of % relative standard deviation (% RSD) (eqn (7)).

$$\sigma \ (SD) = \sqrt{\frac{1}{N-1} \times \sum_{i=1}^{N} \left(x_i - \overline{X}\right)^2} \tag{6}$$

where, 'σ' is standard deviation, 'x_i' is concentration values, and '$\overline{X}$' is the average value.

$$\% \ RSD = \frac{\sigma}{\overline{X}} \times 100 \tag{7}$$

3.1.2.1 Z-score and zeta score.

The Z or zeta score indicates how many times the determined concentration is of the population mean. It is always measured at the 95.5% confidence interval and is given as follows.

$$Z \ score = \left.\frac{\overline{X} - \mu}{\sigma}\right\}$$

when, $|z| = \pm 1$: then results are good
if $1 < |z| \leq 2$: results are acceptable and need to be checked
$2 < |z| \geq 3$: results are questionable and not acceptable
$$\tag{8}$$

where '$\overline{X}$' is laboratory mean value, 'μ' is population mean, and 'σ' is population uncertainty. The zeta score can be expressed as

$$Zeta \ score = \left|\frac{\overline{X} - \mu}{\sqrt{u_{exp}^2 + u_{ref}^2}}\right| \tag{9}$$

The zeta score is always a positive value and it involves the total uncertainties (± 2 s, *i.e.*, at 95.5% confidence level) arising due to the experimental and reported uncertainties of the reference material.

3.1.3 Method validation as part of quality control (QC).

The analytical methods were validated using USGS CRMs, namely, G-2, RGM-1, and NIST SRM 610 as control samples and USGS CRM STM-1 was used as the reference standard. CRM G-2 was analyzed by ED-XRF and DC Arc AES, whereas CRM RGM-1 and SRM 610 were analyzed by INAA. These CRMs/SRM were chosen for method validation with the idea that these all have almost similar composition to that of automobile windshield/soda-lime glass. Table 4 summarizes the absolute concentration (mg kg^{-1} or wt%) values, certified values, and zeta-score of analytes in USGS G-2 analyzed by the DC Arc AES and ED-XRF methods. The zeta-score values (calculated from eqn (9)) for all major and minor elements were found to be closer to 1 (at the 95% confidence level). In case of the zeta score, the large uncertainties on the estimated results have been taken care of along with the reported uncertainties in the certified values. From the zeta score values, it can be concluded that both methods are suitable for the estimation of major and minor elements including transition elements. The uncertainties in the results have been expressed (at ± 1 s) and obtained from replicate sample analysis ($n = 3$); the results indicated that these two methods suffer from relatively poor precision (% RSD varied from 5–13%) compared to INAA.

In our earlier work,[8] we analyzed USGS CRM G2 by INAA for almost all elements of interest and the % deviations and Z-score values (at 95.5% confidence level) were found to be within $\pm 10\%$ and ± 1, respectively. In view of this, we have taken other reference materials, namely, USGS CRM RGM-1 as well as glass

Table 4 A comparative evaluation of experimentally determined concentration (mg kg^{-1} or % unless mentioned) of the analytes in USGS G-2, their certified values, and zeta-score using DC Arc AES and ED-XRF methods[a]

| Element/oxide | Certified values | USGS G-2 (granite) | | | |
| | | DC Arc AES | | ED-XRF | |
		Present work	Zeta-score	Present work	Zeta-score
SiO$_2$ (%)	69.14 ± 0.30	68.9 ± 5.6	0.02	69.8 ± 3.6	0.1
Na$_2$O (%)	4.08 ± 0.13	4.4 ± 0.5	0.4	3.8 ± 0.2	0.8
CaO (%)	1.96 ± 0.08	1.8 ± 0.1	0.7	2.08 ± 0.03	0.9
Sc	3.5 ± 0.4	3.9 ± 0.5	0.4	<35 ppm	—
Fe$_2$O$_3$ (%)	2.66 ± 0.17	2.9 ± 0.2	0.6	2.3 ± 0.1	1.2
Co	4.6 ± 0.7	5.0 ± 0.5	0.3	<30 ppm	—
Zn	86 ± 8	73 ± 10	0.7	75 ± 2	0.9
Rb	170 ± 3	ND	—	ND	—
Zr	309 ± 35	260 ± 35	0.7	250 ± 10	1.1
Ba	1880 ± 23	1740 ± 68	1.4	1790 ± 35	1.2
La	89 ± 8	80 ± 7	0.5	92 ± 4	0.21
Hf	7.9 ± 0.7	ND	—	ND	—
Ce	160 ± 10	180 ± 22	0.5	150 ± 8	0.5
Eu	1.4 ± 0.12	<60 ppm	—	<30 ppm	—
Yb	0.8 ± 0.2	<90 ppm	—	<27 ppm	—
Sm	7.2 ± 0.7	<68 ppm	—	<35 ppm	—
Th	25 ± 2	ND	—	ND	—
Sr	478 ± 2	550 ± 45	0.80	420 ± 20	1.4

[a] ND – not detected.

Table 5 Determined concentration (mg kg^{-1} or % wherever mentioned) of the element or oxide in USGS RGM-1 (rhyolite), their certified values, and Z-score by the relative INAA method[a]

Element/oxide	Activation product	Energy (keV)	USGS RGM-1 (rhyolite, glass mountain)			
			Result obtain	Certified value	% dev	Z-score
SiO$_2$ (%)[b]	^{28}Si(p,p')^{28}Si	1779	72.9 ± 0.8	73.4 ± 0.5	−0.7	−0.9
Na$_2$O (%)	^{24}Na	1368.5	3.99 ± 0.09	4.07 ± 0.15	−1.8	−0.5
CaO (%)	^{47}Ca	159.4	1.19 ± 0.02	1.15 ± 0.07	3.5	0.6
Sc	^{46}Sc	1120.9	4.44 ± 0.25	4.4 ± 0.3	0.9	0.1
Cr	^{51}Cr	320	3.74 ± 0.07	3.7	1.2	—
Fe$_2$O$_3$ (%)	^{59}Fe	1292	1.79 ± 0.06	1.86 ± 0.03	−3.8	−2.3
Co	^{60}Co	1332.9	2.05 ± 0.08	2.0 ± 0.2	2.6	0.3
Zn	^{65}Zn	1115.9	34.3 ± 1.7	32	7	—
Rb	^{86}Rb	1077.2	142 ± 2	150 ± 8	−5.3	−1
Zr	^{95}Zr	757	232 ± 14	220 ± 20	5.5	0.6
Ba	^{131}Ba	496.3	824 ± 7	810 ± 46	1.7	0.3
La	^{140}La	1596	24.9 ± 1.3	24.0 ± 1.1	4.1	0.9
Hf	^{181}Hf	482	5.58 ± 0.25	NA	—	—
Ce	^{141}Ce	145.6	44.6 ± 1.4	47 ± 4	−5.1	−0.6
Eu	^{152}Eu	1408	0.71 ± 0.03	0.66 ± 0.08	7	0.6
Yb	^{169}Yb	197.9	2.64 ± 0.16	2.6 ± 0.3	1.4	0.1
Sm	^{153}Sm	102.9	4.4 ± 0.2	4.3 ± 0.3	2.3	0.3
Th	^{233}Pa	312	13.9 ± 0.6	15 ± 1.3	−6.8	−0.8

[a] NA: not available. [b] SiO$_2$ was determined by the PIGE method.

reference material NIST SRM 610 (sodalime glass), for the method validation of INAA. The analytical results of RGM-1 are given in Table 5. Seventeen elements (Na, Ca, Sc, Cr, Fe, Co, Zn, Rb, Zr, Ba, La, Hf, Ce, Eu, Yb, Sm, and Th) determined at major, minor, and trace concentration levels by this method were found to be in good agreement (within ±5% deviation) with the corresponding certified values. The Z-score as well as zeta score values (calculated using eqn (8) and (9), respectively) were found to be within ±1 (at 95.5% confidence level) for almost all the analytes, except for Fe. The uncertainties (±1 s) reported in the concentration of INAA results (in Table 5) were found to be in the range from ±1.5% to ±6%, which are expressed as standard deviation obtained from replicate ($n = 3$) sample analysis. SiO$_2$ concentration in USGS RGM-1 (CRM) was determined through the analysis of the sample in the pellet form through conventional (in vacuum chamber) *in situ* current normalized Particle Induced Gamma-ray Emission (PIGE) method using F as an *in situ* current normalizer. In this method, the target samples were irradiated with 4 MeV proton beam ($I \sim 10$–15 nA) from Folded Tandem Ion Accelerator (FOTIA) and the measurement of prompt gamma rays emitted from ^{28}Si(p,p')^{28}Si reaction was carried out using high resolution gamma ray spectrometry with HPGe detector. Detailed sample preparation, methodology, and experimental part can be found in our earlier publications.[8,54,58] The Si result was also found to be in good agreement with the certified values and uncertainties in the results, expressed at ±1 s, which were found to be about ±1% (Table 5). The reported uncertainty in the Si concentration was also calculated from the replicate ($n = 3$) sample analysis and has contribution from standard deviation.

The certified reference material for glass sample NIST SRM 610 was analyzed by INAA in five replicates, and the results were compared with the certified values. The % relative standard deviation (% RSD) and % deviation were measured for all the analyte and are summarized in Table 6.

3.1.4 Analysis of automobile windshield glass samples. The compositional characterization of six different automobile glass samples (GA to GF) was carried out in the present investigation. A total of eight elements including four major (Si, Na, Ca, and Fe) and four minor (Cr, Zn, Zr, and Sr) elements were found to be present, as suggested by the ED-XRF analysis. The absolute concentration (wt% or mg kg^{-1}) along with standard deviation (at ±1 s) from replicate sample analysis are summarized in Table 7. The uncertainties in the results are found to vary from ±5% to 10%, which are due to the standard deviation from replicate ($n = 3$) sample analysis. The analytes, namely, Sc, Co, Ba, La, Ce, Eu, Yb, and Sm, were found to be below the limits of detection in all automobile glass samples.

The concentration of ten elements including four major and six minor and trace elements, namely, Si, Na, Ca, Fe, Cr, Co, Zn, Zr, Ba and Sr were quantified by the DC Arc AES method (Table 8). The obtained uncertainties were expressed at ±1 s and found to vary from ±6% to ±15% (except for Zn, *i.e.*, ±10 to ±20%), which are due to standard deviation from replicate ($n = 3$) sample analysis. The other elements including transition and REEs (Sc, La, Ce, Eu, Yb, Sm) were found to be below the detection limit in all the glass samples since they are known to form refractory oxides at the arc temperature and are unable to be swept out of the matrix completely.[48–50] The analytes such as Rb, Hf, and Th were not analyzed by the DC Arc AES method. The analytical method should be user-friendly, non-destructive, and provide unambiguous results with adequate accuracy and precision, which are prime requirements for forensic applications.[60] ED-XRF and DC Arc AES are widely used lab-based

Table 6 Analysis of certified reference material for glass NIST SRM 610 by INAA in five replicates

Element	NIST SRM 610			
	Certified	Present work (mean ± std)	% RSD ($n = 5$)	% deviation
SiO_2 (%)[a]	72	71.2 ± 0.8	1.1	−1.1
Na (%)	10.4	10.1 ± 0.1	1.2	−2.9
Ca (%)	8.57	8.47 ± 0.30	3.6	−1.2
Sc	441 ± 9.6[b]	438 ± 20	4.5	−0.7
Cr	415 ± 29	402 ± 14	3.4	−3.1
Fe	458 ± 9	446 ± 7	1.7	−2.5
Co	390	402 ± 13	3.4	3.0
Zn	433	457 ± 28	6.1	5.6
Rb	425.7 ± 0.8	423 ± 9	2.1	−0.7
Zr	439.9 ± 7.8[b]	443 ± 18	4.1	0.7
Cs	360.9 ± 67.5[b]	363 ± 11	3.1	0.5
Ba	453 ± 37	432 ± 11	2.5	−4.4
La	457.4 ± 72.4[b]	445 ± 19	4.3	−2.7
Hf	417.7 ± 28.2[b]	425 ± 13	3.0	1.7
Ce	447.8 ± 16.8[b]	449 ± 24	5.5	0.4
Eu	461.1 ± 52.1[b]	456 ± 19	4.1	−1.1
Yb	461.5 ± 30.6[b]	455 ± 36	7.9	−1.5
Sm	450.5 ± 20.6[b]	456 ± 37	8.2	1.2
Th	457.2 ± 1.2	455 ± 2	0.3	−0.5

[a] SiO_2 was determined from Particle Induced Gamma-ray Emission (PIGE), standard mean and standard deviation were estimated from replicate analyses. [b] Concentration values were taken from the literature values from ref. 59.

Table 7 Determined elemental concentration of automobile glass samples by the ED-XRF method

Element/oxide	GA	GB	GC	GD	GE	GF
SiO_2 (%)	73.5 ± 3.8	71.1 ± 3.9	70.8 ± 3.5	74.1 ± 4.1	72.7 ± 3.6	74 ± 4
Na_2O (%)	12.9 ± 0.8	13 ± 1	13.3 ± 0.9	11 ± 1	12.3 ± 1.2	11 ± 1
CaO (%)	4.0 ± 0.3	4.8 ± 0.3	4.7 ± 0.4	10 ± 1	6.0 ± 0.6	8.1 ± 0.8
Cr (mg kg^{-1})	36 ± 2	<28	<28	38 ± 3	<28	<28
Fe_2O_3 (%)	0.40 ± 0.02	0.49 ± 0.02	0.49 ± 0.02	0.61 ± 0.02	0.51 ± 0.02	0.53 ± 0.02
Zn (mg kg^{-1})	35 ± 3	<27	<27	<27	<27	<27
Zr (mg kg^{-1})	50 ± 4	60 ± 4	65 ± 4	102 ± 10	77 ± 5	61 ± 4
Sr (mg kg^{-1})	50 ± 5	72 ± 5	45 ± 5	68 ± 6	70 ± 6	55 ± 5

techniques having many favorable characteristics. In the present context, particularly for this type of samples (glass/ceramics), the technique such as INAA is more suitable for the quantification of trace elements including rare earth elements (REEs) compared to these two techniques and is also capable of analyzing direct glass/glass powder without any matrix effect.

INAA was employed to all six automobile glass samples to determine major, minor, and trace elements, including transition and rare earth elements. A total of eighteen elements (Na, Ca, Sc, Cr, Fe, Co, Zn, Rb, Zr, Cs, Ba, La, Hf, Ce, Eu, Yb, Sm, and Th) were quantified, and the results are summarized in Table 9. The uncertainties (at ±1 s) were found to vary in the range of ±1.5–6% for all the elements, which are due to the standard deviation from replicate ($n = 3$) sample analysis. The concentration range of REEs (La, Ce, Eu, Yb, and Sm) were found to be as follows: La (1.34–8.56 mg kg^{-1}), Ce (4.51–16.8 mg kg^{-1}), Sm (0.30–1.15 mg kg^{-1}), Eu (0.19–0.29 mg kg^{-1}), and Yb (0.24–0.71 mg kg^{-1}) (Table 9). Since Si was not determined by INAA, we have employed *in situ* current normalized Particle Induced

Gamma-ray Emission (PIGE) method to obtain the complete compositional idea of the above analyzed automobile glass samples.[8] The SiO_2 concentrations were found to vary in the range from 70.5–73.9% (Table 9), which were found to be in agreement with the concentration obtained from the other two methods, *i.e.*, ED-XRF and DC Arc AES methods. The uncertainties in the concentration results for all six glasses obtained by the PIGE method were found to vary from ±0.5% to ±1.3% (at ±1 s), which are also due to replicate ($n = 3$) sample analysis. From the concentration results, it can be concluded that four elements, namely, Si, Na, Ca, and Fe, constitute the major matrix, and these all were found to be present at the % level in all the analyzed glass samples. Beside this, it can also be stated that these automobile glass samples are of sodalime class of glasses as these values are in close agreement with the literature data for automobile (soda-lime) glasses.[8] The elemental concentration, total transition elements and total REEs, and their ratio were utilized for the preliminary grouping of six automobile glass samples for potential forensic applications, as

Table 8 Determined elemental concentrations of six automobile glass samples by the DC Arc carrier distillation AES method

Element/oxide	GA	GB	GC	GD	GE	GF
SiO_2 (%)	72.9 ± 6.8	71.2 ± 6.4	69.5 ± 7.2	73.4 ± 6.9	72.9 ± 6.1	73.8 ± 7.5
Na_2O (%)	14 ± 1	13 ± 1	14 ± 1	13 ± 1	13 ± 1	12 ± 1
CaO (%)	4.3 ± 0.4	4.2 ± 0.4	4.4 ± 0.4	8.3 ± 0.5	5.2 ± 0.5	7.2 ± 0.6
Cr (mg kg^{-1})	40 ± 4	<5	<5	41 ± 4	<5	<5
Fe_2O_3 (%)	0.52 ± 0.08	0.50 ± 0.06	0.52 ± 0.06	0.60 ± 0.06	0.52 ± 0.05	0.49 ± 0.05
Co (mg kg^{-1})	10 ± 1	8 ± 1	<4	<4	<4	<4
Zn (mg kg^{-1})	30 ± 3	15 ± 2	10 ± 2	10 ± 2	<7	15 ± 2
Zr (mg kg^{-1})	<90	<90	<90	93 ± 10	<90	<90
Ba (mg kg^{-1})	40 ± 4	40 ± 4	50 ± 5	20 ± 3	20 ± 3	50 ± 5
Sr (mg kg^{-1})	58 ± 4	70 ± 6	48 ± 5	62 ± 6	66 ± 6	60 ± 5

Table 9 Determined elemental concentrations of six different automobile glass samples by the relative INAA method

Element/oxide	GA	GB	GC	GD	GE	GF
SiO_2 (%)[a]	73.9 ± 0.5	70.9 ± 0.6	71.6 ± 0.5	70.8 ± 0.5	70.5 ± 0.9	72.2 ± 0.4
Na_2O (%)	13.4 ± 0.2	11.6 ± 0.2	12.9 ± 0.2	13.2 ± 0.3	12.4 ± 0.3	11.7 ± 0.3
CaO (%)	3.75 ± 0.07	5.08 ± 0.12	5.12 ± 0.12	8.80 ± 0.21	6.18 ± 0.14	7.61 ± 0.18
Sc (mg kg^{-1})	0.51 ± 0.03	1.45 ± 0.08	1.28 ± 0.07	0.25 ± 0.01	0.75 ± 0.04	1.35 ± 0.08
Cr (mg kg^{-1})	35.2 ± 0.5	2.77 ± 0.05	3.35 ± 0.06	42.7 ± 0.6	2.93 ± 0.05	6.09 ± 0.11
Fe_2O_3 (%)	0.48 ± 0.02	0.49 ± 0.02	0.49 ± 0.02	0.67 ± 0.02	0.49 ± 0.02	0.53 ± 0.02
Co (mg kg^{-1})	8.80 ± 0.42	5.34 ± 0.29	3.69 ± 0.19	2.20 ± 0.12	2.00 ± 0.11	3.37 ± 0.18
Zn (mg kg^{-1})	31 ± 1	14.8 ± 0.7	11.4 ± 0.6	9.95 ± 0.54	3.18 ± 0.17	14.1 ± 0.7
Rb (mg kg^{-1})	8.76 ± 0.17	13.8 ± 0.2	17.5 ± 0.3	15.2 ± 0.3	39.2 ± 0.5	19.3 ± 0.4
Zr (mg kg^{-1})	55 ± 2	60 ± 2	65 ± 2	102 ± 6	77 ± 3	61 ± 2
Cs (mg kg^{-1})	0.45 ± 0.02	0.22 ± 0.01	0.39 ± 0.02	0.42 ± 0.02	1.94 ± 0.12	0.39 ± 0.02
Ba (mg kg^{-1})	36.4 ± 0.7	41.4 ± 0.8	58 ± 1	22.3 ± 0.6	26.6 ± 0.5	50.7 ± 1.4
Hf (mg kg^{-1})	1.29 ± 0.06	1.41 ± 0.06	1.29 ± 0.06	2.54 ± 0.11	2.07 ± 0.09	1.59 ± 0.07
La (mg kg^{-1})	1.34 ± 0.07	6.23 ± 0.31	3.98 ± 0.21	8.56 ± 0.49	5.26 ± 0.28	8.04 ± 0.44
Ce (mg kg^{-1})	4.51 ± 0.14	7.43 ± 0.24	7.94 ± 0.25	16.8 ± 0.4	8.93 ± 0.28	7.64 ± 0.31
Sm (mg kg^{-1})	0.30 ± 0.01	0.88 ± 0.04	0.70 ± 0.03	1.15 ± 0.06	0.67 ± 0.03	0.99 ± 0.05
Eu (mg kg^{-1})	0.20 ± 0.01	0.28 ± 0.01	0.29 ± 0.01	0.27 ± 0.01	0.19 ± 0.01	0.25 ± 0.01
Yb (mg kg^{-1})	0.24 ± 0.01	0.71 ± 0.02	0.47 ± 0.02	0.53 ± 0.03	0.68 ± 0.04	0.61 ± 0.04
Th (mg kg^{-1})	1.21 ± 0.05	1.24 ± 0.05	1.53 ± 0.06	3.47 ± 0.14	2.68 ± 0.11	1.85 ± 0.07
Total REE (mg kg^{-1})	6.59	15.5	13.4	27.3	15.7	17.5
Total transition elements except Fe (mg kg^{-1})	132	86	86	160	88	88

[a] SiO_2 was determined from Particle Induced Gamma-ray Emission (PIGE).

discussed below. Strontium (Sr) was estimated in the glass samples by DC Arc AES and ED-XRF. However, INAA cannot determine Sr as it forms short-lived activation product on bombardment with neutron. To estimate Sr by NAA, prompt gamma neutron activation analysis is required, where online measurement of gamma ray from compound nucleus can be used for Sr quantification.

3.1.5 Investigation of the interday variation in the analytical results. In DC Arc carrier distillation AES technique, 5% AgCl was used as a carrier to sweep away the analytes into the arc. Since the amount of Ag taken for all the replicate measurement is effectively same, so the variation is mainly govern by the arc characteristics which is different each arc. Keeping this in view, the calibration curves for each analyte were established based on the intensity ratio of the analyte with respect to Ag. This strategy normalizes all the day-to-day and arc-to-arc variations.[48–50] This strategy is well known and adopted worldwide. In the present case also, the same strategy was followed to take care of such variations. Same samples and standards (mixed with AgCl) were also used for ED-XRF analysis, and intensity ratio with respect to Ag was utilized for normalization in the calibration curves; hence, the variations were taken care of. Moreover, all our analytical techniques are relative in nature and each time while analyzing the sample, standards were also analyzed. Hence, the day-to-day variation would modify the calibration curve and the elemental estimation would be taken care of. This variation can be a problem and is needed to be corrected only when the analysis of standard and samples are done in different days. But the scenario is not same for the present investigation, as specified earlier. The interday variation in the analytical data for the sample 'GA' obtained by DC Arc AES and ED-XRF are depicted in Fig. 5, which indicates that even though there was a small variation in the data, the data are found to be within the error limit specified earlier, meaning that the variation in interday analysis is found to be within the acceptable statistical fluctuation.
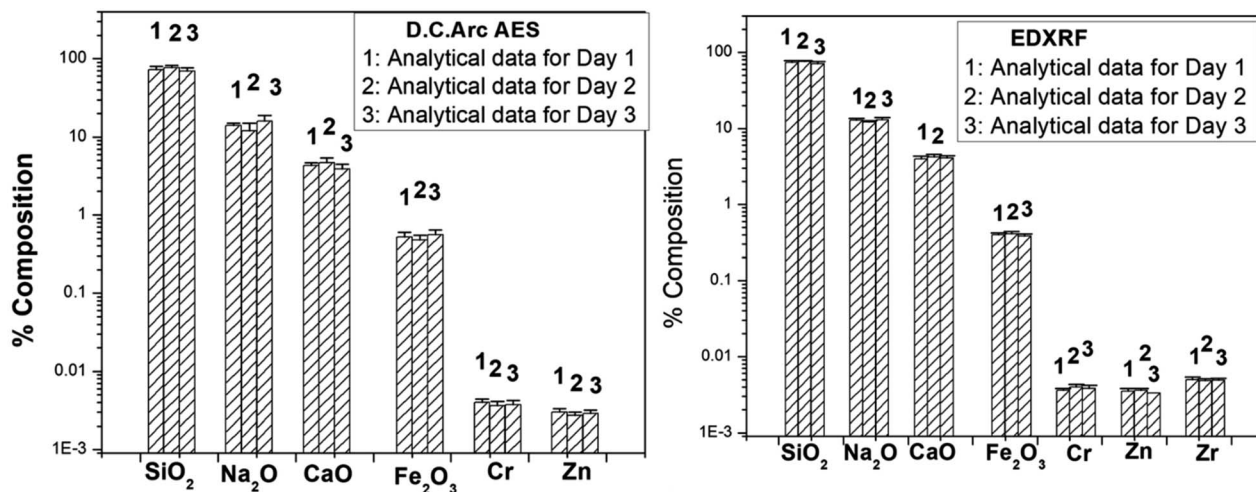
Fig. 5 The variation in the analytical data obtained by the analysis of the GA sample at three different days by DC Arc AES and ED-XRF.

3.1.6 Toward trace evidence (less mass) analysis for accomplishing the need of forensics. In case of DC Arc AES and ED-XRF, the above sample size was kept the same for achieving the detection limits and the confidence interval associated with each data point. It is believed that the sampling would be very important for a small sample size if the samples are not homogeneous. A small sample size may be used for DC Arc AES and ED-XRF; however, there would be a compromise in the precision on the results. This work is focused on the analytical capabilities with the standard sample size required for each technique. In real forensic cases, often smaller fragments or size samples of a few mg are obtained and a very few techniques can perform forensic trace evidence analysis where results are obtained with

higher uncertainties as the main purpose is evidence identification. In view of that, attempts were made for the characterization of one representative (GA) sample with 2 mg sample size using INAA and DC Arc AES (by mixing with the carrier). The analytical results are given in Table 10. The results obtained here are not from a representative sample mass but important information in terms forensic investigation can be obtained from the results. The obtained results indicated that INAA using high neutron flux is a very useful tool for trace evidence analysis as it could give maximum chemical information compared to other methods, *i.e.*, ED-XRF and Dc Arc AES.

3.1.7 Grouping of automobile windshield glass samples using major and minor elements obtained through ED-XRF and DC Arc AES methods. Major elemental (Si, Na, Ca, Fe) concentration results of analyzed glass samples revealed that these automobile glasses are sodalime glasses (as discussed in Section 3.1.4). The preliminary grouping of these analyzed glasses was carried out by comparing the elemental concentrations and also through the presence/absence of the elements. Out of these four major elements, concentrations of Ca and Fe were found to be high for GD as compared to the other five glass samples, indicating that glass GD is quite different from others. The concentration results obtained through ED-XRF also revealed that the concentration of major elements (Ca & Fe) and minor elements (Cr & Zr) is significantly high for GD glass, whereas the presence of Zn in GA glass could differentiate GA from other four glass samples (GB, GC, GE, GF) (Table 7). Thus, presence/absence of Zn and relatively higher concentration of major and minor elements (Ca, Fe, Cr, and Zr) could be utilized to differentiate these glass samples for forensic application. The ED-XRF results indicated that the six glasses fall into three major groups: (Group A) GA; (Group B) GB, GC, GE & GF; and (Group C) GD.

On the other hand, the DC Arc AES method could give more elemental information than ED-XRF, but the associated % RSD (relative standard deviations) were found to be quite high (6–15%) (Table 8). Besides this, it could differentiate the GD from

Table 10 The effect of lower sample size (2 mg) on the analyses of glass samples by INAA and DC Arc AES[a]

Element/oxide	INAA	DC Arc AES
Na$_2$O (%)	13.5	15
CaO (%)	4.0	4.5
Sc (mg kg^{-1})	0.55	NA
Cr (mg kg^{-1})	35	39
Fe$_2$O$_3$ (%)	0.50	0.55
Co (mg kg^{-1})	9.0	ND
Zn (mg kg^{-1})	31	37
Rb (mg kg^{-1})	8.76	NA
Zr (mg kg^{-1})	50	ND
Cs (mg kg^{-1})	0.44	NA
Ba (mg kg^{-1})	36	34
Hf (mg kg^{-1})	1.3	NA
La (mg kg^{-1})	1.4	ND
Ce (mg kg^{-1})	4.6	ND
Sm (mg kg^{-1})	0.30	ND
Eu (mg kg^{-1})	0.25	ND
Yb (mg kg^{-1})	0.25	ND
Th (mg kg^{-1})	1.20	ND
Sr (mg kg^{-1})	ND	60

[a] ND: not detected; NA: not analyzed.

all other five glass samples through the elemental concentration of major (Ca) and minor (Cr, Zr, & Ba) elements.

Statistical Cluster Analysis (CA) is an efficient method for grouping study of similar kind of materials and has been extensively utilized for the grouping of pottery for archaeological and glass samples in forensic applications.[54,61–64] In this view, the grouping pattern of the analyzed glass samples was confirmed by performing independent cluster analysis (CA) utilizing major and minor elemental concentrations obtained by ED-XRF and DC Arc AES methods; the corresponding tree diagrams are shown in Fig. 6 and 7, respectively. In case of ED-XRF, the analyzed glass samples were found to be fall into three groups, i.e., Group A (GA); Group B (GB, GC and GE); and Group C (GD and GF). On the other hand, with the DC Arc AES data, the obtained pattern was found to be different, and the three groups are Group A (GA and GC); Group B (GB, GF, and GE); and Group C (GD). Although both DC Arc AES and ED-XRF data could group the all the six analyzed glass samples into the three different groups, but the obtained grouping patterns are found to be different in each case and are not in concurrence with the expected (actual) grouping pattern. To confirm the grouping
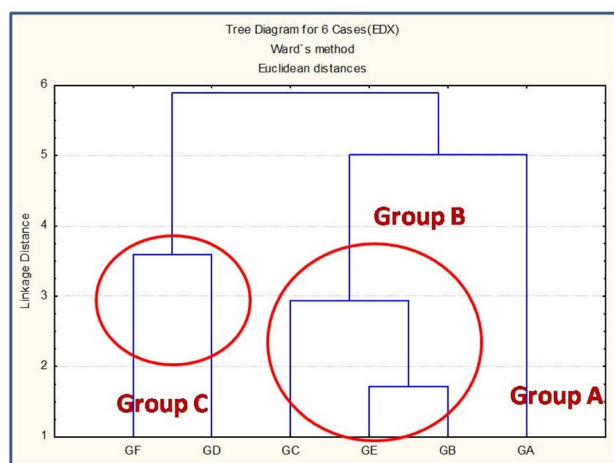
Fig. 6 Cluster analysis using elemental concentration data by ED-XRF.
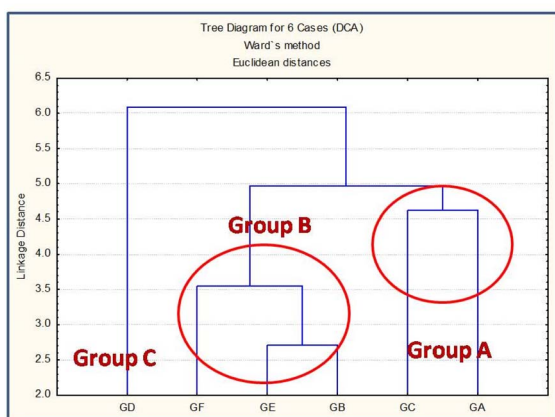
Fig. 7 Cluster analysis using elemental concentration data by DC Arc AES.

patterns obtained by ED-XRF or DC Arc AES methods utilizing major and minor elemental concentration, CA was also employed using INAA data, as discussed in the subsequent section.

3.1.8 Grouping study utilizing transition elements and rare earth elements (REEs) concentrations obtained through the INAA method and confirmation of possible groups through statistical analysis. Elemental profiling of all the samples (Fig. 8(a)) confirmed the appreciable variation in minor and trace elements, including transition and rare earth elements (REEs) compared to major elements. In addition, some trace elements, namely, La and Ce, were found to have significantly larger variation than others (Fig. 8(b)). Hence, REEs can be used as key markers or signature elements for grouping and finding the source of the glass samples. Sharma et al. (2019) have demonstrated the importance of REEs in the grouping of automobile glass samples. They have utilized the elemental concentration ratio (La/Ce) and total REEs (sum of obtained REE concentration) for the grouping of glass samples.[8] Dasari et al. (2012, 2013, and 2018) and Sharma et al. (2022) have used minor and trace elemental concentrations for the provenance studies of some archeological artifacts, including bricks, pottery samples, and glass forensics, respectively.[61–64] Nakanishi et al. (2008) have used Ba and La intensity ratio and presence/absence of elements (Hf, Pb, and Mo) for the grouping of glass fragments.[45] Compared to major elements, the transition elements and REEs mostly present at trace levels, i.e., less than 100 ppm, are source-specific in nature.[65,66] Consequently, their concentrations or concentration ratios in raw materials and finished products do not vary and were utilized for provenance studies.[67] The total REE concentrations for all the six automobile glass samples are plotted in Fig. 8(c) and reveal that the glasses (GB, GC, GE, & GF) are different from the other two glass samples (GA and GD). Further, total REEs concentration for glass (GA) was found to be the lowest and for glass (GD), it was significantly high. Thus, from the REEs concentration, these six glass samples could be categorized into three groups (Group A (GA), Group B (GB, GC, GE, and GF), and Group C (GD)). The elemental concentration of some major (Ca, Fe), minor (Zr), and trace (Sc, Ce, Sm) elements were found to be high in glass GD compared to other glasses, whereas transition elements (Co, Zn) were found to be present in relatively high concentration. On the other hand, in GA glass, elements such as Zr and Sm were found to be at a lower level, which could help in differentiating the GA and GD glasses from the other four glasses. Elemental concentration ratios, namely, La/Sc, Ce/Sc, total REEs (La + Ce + Eu + Yb + Sm) and total transition elements (Sc + Cr + Co + Zn + Zr + Hf), which were present at trace concentration levels, also supported our preliminary grouping that automobile glass (GD) is totally different from all other five automobile glass samples (GA to GC & GE to GF), whereas among these five glasses, four glasses (GB, GC, GE, & GF) were found to be different than glass GA (Table 8). INAA results also indicated that all six glasses fall in three groups: Group A (GA); Group B (GB, GC, GE & GD); and Group C (GD).

Further, statistical cluster analysis was carried out to confirm the preliminary grouping obtained from the INAA results and
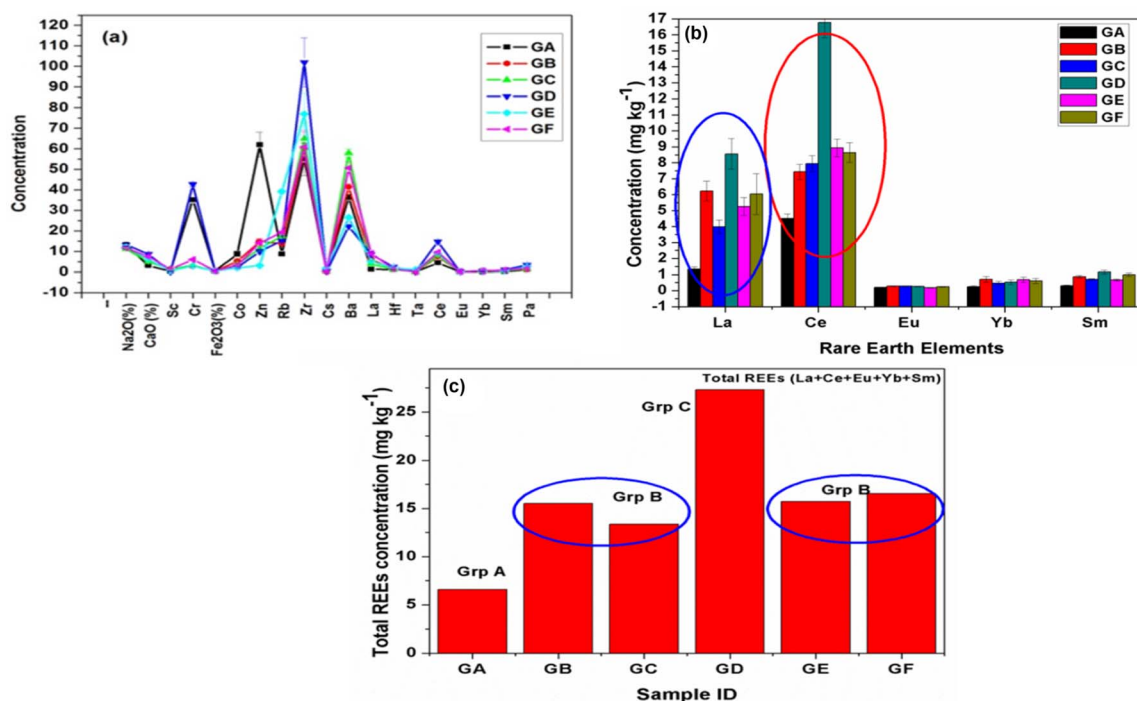
Fig. 8 (a) Elemental profile in six glass samples; (b) concentration *vs.* REEs bar plot for six glass samples; (c) total REEs in all six glass samples.

also to solve the ambiguity in the grouping pattern obtained in case of ED-XRF and DC Arc AES using major and minor elements. In this view, the elemental concentration of twelve minor and trace elements including transition and rare earth elements (Sc, Cr, Fe, Co, Zn, Zr, La, Hf, Ce, Eu, Yb, and Sm) obtained by the INAA method were utilized for cluster analysis employing Ward's agglomeration method for confirming the grouping pattern obtained through the extensive analysis of the data obtained through all the three used methods, *i.e.*, ED-XRF, DC Arc AES, and INAA. Fig. 9 shows the tree dendogram obtained for six automobile glass samples using minor and trace elemental concentrations obtained by the INAA method. The

analyzed glass samples broadly fall into three groups, *i.e.*, Group A (GA), Group B (GB, GC, GE, GF), and Group C (GD). It is clear from the CA dendogram that GD is quite different due its different source, and among the other five, GA is different from GB, GC, GE, & GF. These findings also support our preliminary grouping, as discussed above and in Section 3.1.7.

The grouping pattern obtained in the case of INAA was found to be different from those obtained by the ED-XRF and DC Arc AES methods. The major difference was observed in the Euclidean distance (*y*-axis) of the dendograms obtained by all the three methods (Fig. 6, 7, and 9). In case of ED-XRF and DC Arc AES methods, it was found to reduce to 5 to 6 units compared to the INAA tree diagram, where it is about 25 units. The decrease in the Euclidean distance indicated that there are more similarities in the data set used for the grouping studies. Most of the elements (Si, Na, Ca, and Fe) determined by both ED-XRF and DC Arc AES methods were found to be present at the % level with no significant differences in their concentrations which leads to a reduction in the Euclidean distance. On the other hand, minor and trace elements determined by INAA methods have showed more variations for the analyzed glass samples (Fig. 8(a and b)) and can be utilized as key markers or diagnostic elements, which results in more Euclidean distance in the tree diagram (Fig. 9). Secondly, INAA could provide more elemental concentration data including trace elements, which are source-specific in nature, which led to more authentic grouping pattern through the statistical cluster analysis. This study highlights the role of the minor and trace elements obtained by INAA for the grouping study of automobile windshield glass samples for possible forensic applications. In conclusion, minor and trace elemental concentrations in conjunction with
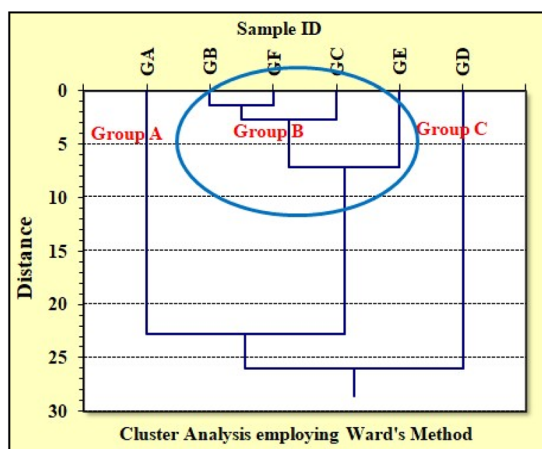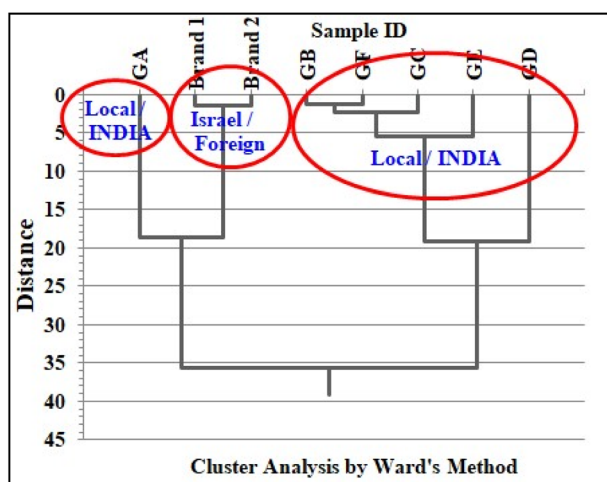

Fig. 9 Cluster analysis utilizing minor and trace elemental concentration of six different automobile glass employing Ward's method.
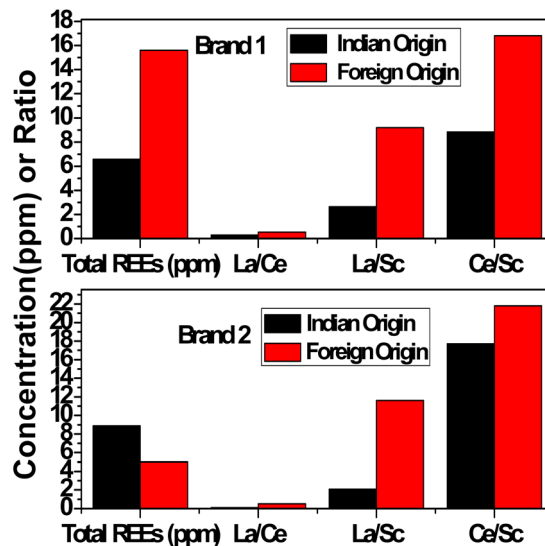
Table 11 Minor and trace elemental concentration of typical two different brands belonging to Indian and foreign origin

Element/oxide	Brand 1		Brand 2	
	Indian	Foreign	Indian	Foreign
Sc (mg kg^{-1})	0.51 ± 0.03	0.56 ± 0.06	0.39 ± 0.02	0.14 ± 0.02
Cr (mg kg^{-1})	35.2 ± 0.5	2.38 ± 0.06	3.95 ± 0.09	2.72 ± 0.09
Fe$_2$O$_3$ (%)	0.48 ± 0.02	0.48 ± 0.01	0.18 ± 0.01	0.51 ± 0.01
Co (mg kg^{-1})	8.80 ± 0.42	5.51 ± 0.12	1.02 ± 0.08	0.33 ± 0.02
Zn (mg kg^{-1})	31 ± 1	<2.2	68.3 ± 3.7	<2.2
Rb (mg kg^{-1})	8.76 ± 0.17	10.4 ± 0.6	6.59 ± 0.21	<2
Zr (mg kg^{-1})	55 ± 2	65.7 ± 6.9	<19	24.7 ± 2.1
Ba (mg kg^{-1})	36.4 ± 0.7	39.3 ± 4.3	67.6 ± 1.4	<1.3
La (mg kg^{-1})	1.34 ± 0.07	5.13 ± 0.22	0.82 ± 0.04	1.62 ± 0.09
Hf (mg kg^{-1})	1.29 ± 0.06	1.95 ± 0.14	0.79 ± 0.04	0.49 ± 0.04
Ce (mg kg^{-1})	4.51 ± 0.14	9.42 ± 0.66	16.9 ± 0.5	3.05 ± 0.22
Eu (mg kg^{-1})	0.20 ± 0.01	0.17 ± 0.02	0.18 ± 0.01	0.08 ± 0.01
Yb (mg kg^{-1})	0.24 ± 0.01	0.20 ± 0.02	0.35 ± 0.04	0.05 ± 0.01
Sm (mg kg^{-1})	0.30 ± 0.02	0.70 ± 0.05	0.63 ± 0.03	0.22 ± 0.02
Total REEs	6.59	15.6	8.89	5.02
La/Ce	0.29	0.54	0.12	0.53
La/Sc	2.63	9.2	2.10	11.6
Ce/Sc	8.84	16.8	17.7	21.8

Fig. 11 Bar plot of total REEs (ppm) and ratios such as La/Ce, La/Sc, and Ce/Sc of different automobile glass from India and foreign origin of same brands.

statistical cluster analysis are found to be powerful for grouping similar types of automobile windshield glass samples, which are important forensic evidence in criminal investigations.

To extend our work, automobile glasses of two different origins (local (India)/foreign (Israel)) were analyzed by the INAA method. We are presenting the concentration results of only transition and rare earth elements (REEs) present in automobile glasses of two similar brands of cars having different origins (two from India and two from Israel) (Table 11). The analysis of results clearly indicates that just the presence/absence of elements such as Zn, Zr, and Ba, the elemental concentration results of marker elements, namely, La and Ce, their concentration ratios *i.e.*, La/Ce, La/Sc, and Ce/Sc, and total REEs are

enough to distinguish these similar type of glasses obtained from two different origins. The elemental concentration results of Brand 1 and Brand 2 from foreign origin together with elemental concentration results of all local/Indian glass (GA to GF) were subjected to cluster analysis utilizing all transition elements and REEs similarly, as discussed above (Fig. 10), which clearly distinguished or grouped the two foreign glass samples (Brand 1 and Brand 2) from the Indian car windshield glasses. Further, the bar plots of total REEs and concentration ratios, La/Ce, La/Sc, and Ce/Sc, of two different automobile glasses of Indian and foreign origin of the same brand or manufacture are shown in Fig. 11, which indicated that these two glass samples are from two different sources. This study confirms the source specific nature of trace elements. The aim of this exercise is to show the capability of INAA in conjunction with statistical analysis in distinguishing glass samples having different origins. This exercise actually opens up the scope to perform extensive study in this direction by analyzing more number of samples for possible forensic applications *via* grouping study.

4. Conclusions

A comprehensive investigation of three different analytical techniques, *i.e.*, ED-XRF, DC Arc AES, and INAA, has been presented for the chemical characterization of car windshield glass samples (as important forensic evidence) using solid powder samples. ED-XRF and DC Arc AES methods were found to be good for the determination of major and minor matrix elements; however, INAA showed better performance for the quantification of elements present at the major, minor, and trace levels, including some important marker elements. The elemental concentration of some elements/marker elements such as Fe, Co, Zn, Zr, La, and Ce, concentration ratios such as

Fig. 10 Cluster analysis utilizing minor and trace elemental concentrations of six different automobile glass from India and foreign origin employing Ward's method.

La/Sc and Ce/Sc, sum of REEs, and sum of transition elements could give a fair and preliminary idea for the grouping of similar classes of glass samples. The minor and trace elemental concentration results obtained by INAA in conjunction with statistical cluster analysis were found to be useful for confirming the preliminary grouping among similar types of materials, which is important for possible forensic applications. Another important observation in terms of forensic study is related to the source-specific nature of trace elements, wherein glass samples of the same brand (manufacture) from two different origins (India and Israel) showed different from trace elemental concentrations (both absolute and relative) since their manufacture sources are different. This study highlights the role of minor and trace elements obtained by INAA and cluster analysis in the grouping study of similar types of glasses for glass forensics.

Conflicts of interest

There are no conflicts to declare.

Acknowledgements

References

1 J. C. Mauro, C. S. Philip, D. J. Vaughn and M. S. Pambianchi, *Int. J. Appl. Glass Sci.*, 2014, **5**, 2–15, DOI: **10.1111/ijag.12058**.

2 J. C. Mauro and E. D. Zanotto, *Int. J. Appl. Glass Sci.*, 2014, **5**, 313–327, DOI: **10.1111/ijag.12087**.

3 B. C. Sales and L. A. Boatner, *Science*, 1984, **226**, 45–48, DOI: **10.1126/science.226.4670.45**.

4 C. Kaushik, R. Mishra, P. Sengupta, A. Kumar, D. Das, G. Kale and K. Raj, *J. Nucl. Mater.*, 2006, **358**, 129–138, DOI: **10.1016/j.jnucmat.2006.07.004**.

5 P. Sengupta, K. K. Dey, R. Halder, T. G. Ajithkumar, G. Abraham, R. K. Mishra, C. P. Kaushik and G. K. Dey, *J. Am. Ceram. Soc.*, 2014, **98**, 88–96, DOI: **10.1111/jace.13303**.

6 A. Shortland, N. Rogers and K. Eremin, *J. Archaeol. Sci.*, 2007, **34**, 781–789, DOI: **10.1016/j.jas.2006.08.004**.

7 P. Robertshaw, N. Benco, M. Wood, L. Dussubieux, E. Melchiorre and A. Ettahiri, *Archaeometry*, 2009, **52**, 355–379, DOI: **10.1111/j.1475-4754.2009.00482.x**.

8 V. Sharma, R. Acharya, S. K. Samanta, M. Goswami, H. K. Bagla and P. K. Pujari, *J. Radioanal. Nucl. Chem.*, 2019, **323**, 1451–1457, DOI: **10.1007/s10967-019-06926-7**.

9 G. Zadora, *J. Chemom.*, 2007, **21**, 174–186, DOI: **10.1002/cem.1030**.

10 G. Zadora, *J. Forensic Sci.*, 2009, **54**, 49–59, DOI: **10.1111/j.1556-4029.2008.00905.x**.

11 D. Ramos and G. Zadora, *Anal. Chim. Acta*, 2011, **705**, 207–217, DOI: **10.1016/j.aca.2011.05.029**.

12 J. Hughes, T. Catterick and G. Southeard, *Forensic Sci.*, 1976, **8**, 217–227, DOI: **10.1016/0300-9432(76)90135-7**.

13 J. Henderson, *Archaeometry*, 1988, **30**, 77–91, DOI: **10.1111/j.1475-4754.1988.tb00436.x**.

14 P. Kuisma-Kursula, *X-Ray Spectrom.*, 2000, **29**, 111–118, DOI: **10.1002/(SICI)1097-4539(200001/02)29:1<111::AID-XRS408>3.0.CO;2-W**.

15 Z. Brozel-Mucha, *X-Ray Spectrom.*, 2009, **38**, 58–67, DOI: **10.1002/xrs.1116**.

16 D. C. Duckworth, S. J. Morton, C. K. Bayne, R. D. Koons, S. Montero and J. R. Almirall, *J. Anal. At. Spectrom.*, 2002, **17**, 662–668, DOI: **10.1039/B201575G**.

17 R. D. Koons, C. A. Peters and P. S. Rebbert, *J. Anal. At. Spectrom.*, 1991, **6**, 451–456, DOI: **10.1039/JA9910600451**.

18 A. Zurhaar and L. Mullings, *J. Anal. At. Spectrom.*, 1990, **5**, 611–617, DOI: **10.1039/JA9900500611**.

19 T. Parouchais, I. M. Warner, L. T. Palmer and H. Kobus, *J. Forensic Sci.*, 1996, **41**, 351–360, DOI: **10.1520/JFS13921J**.

20 Ž. Šmit, T. Milavec, H. Fajfar, T. Rehren, J. Lankton and B. Gratuze, *Nucl. Instrum. Methods Phys. Res., Sect. B*, 2013, **311**, 53–59, DOI: **10.1016/j.nimb.2013.06.012**.

21 T. Trejos, S. Montero and J. R. Almirall, *Anal. Bioanal. Chem.*, 2003, **376**, 1255–1264, DOI: **10.1007/s00216-003-1968-0**.

22 T. Trejos and J. R. Almirall, *Anal. Chem.*, 2004, **76**, 1236–1242, DOI: **10.1021/ac0349330**.

23 K. Smith, T. Trejos, R. J. Watling and J. Almirall, *At. Spectrosc.*, 2006, **27**, 69–75, **https://www.speciation.net/Database/Journals/Atomic-Spectroscopy-;i19**.

24 S. Berends-Montero, W. Wiarda, P. D. Joode and G. V. D. Peijl, *J. Anal. At. Spectrom.*, 2006, **21**, 1185–1193, DOI: **10.1039/B606109E**.

25 C. M. Bridge, J. Powell, K. L. Steele and M. E. Sigman, *Spectrochim. Acta, Part B*, 2007, **62**, 1419–1425, DOI: **10.1016/j.sab.2007.10.015**.

26 C. M. Bridge, J. Powell, K. L. Steele, M. Williams, J. M. Macinnis and M. E. Sigman, *Appl. Spectrosc.*, 2006,

60, 1181–1187, https://www.osapublishing.org/as/abstract.cfm?URI=as-60-10-1181.

27 M. M. Suliyanti, M. Pardede, T. J. Lie, K. H. Kurniawan, A. Khumaeni, K. Kagawa, M. O. Tjia and Y. I. Lee, *J. Korean Phys. Soc.*, 2011, **58**, 1129–1134, DOI: 10.3938/jkps.58.1129.

28 N. Miliszkiewicz, S. Walas and A. Tobiasz, *J. Anal. At. Spectrom.*, 2015, **30**, 327–338, DOI: 10.1039/C4JA00325J.

29 N. Carmona, I. Ortega-Feliu, B. Gómez-Tubío and M. Villegas, *Mater. Charact.*, 2010, **61**, 257–267, DOI: 10.1016/j.matchar.2009.12.006.

30 Ž. Šmit, F. Tartari, F. Stamati, A. V. Priftaj and J. Istenič, *Nucl. Instrum. Methods Phys. Res., Sect. B*, 2013, **296**, 7–13, DOI: 10.1016/j.nimb.2012.12.007.

31 S. Chhillar, R. Acharya, R. K. Mishra, C. P. Kaushik and P. K. Pujari, *J. Radioanal. Nucl. Chem.*, 2017, **312**, 567–576, DOI: 10.1007/s10967-017-5251-9.

32 R. F. Coleman and G. C. Goode, *J. Radioanal. Chem.*, 1973, **15**, 367–388, https://link.springer.com/content/pdf/10.1007/BF02516583.pdf.

33 T. Trejos and J. R. Almirall, *Talanta*, 2005, **67**, 388–395.

34 T. Trejos and J. R. Almirall, *Talanta*, 2005, **67**, 396–401, DOI: 10.1016/j.talanta.2005.01.042.

35 J. R. Almirall, *et al.*, *Spectrochim. Acta, Part B*, 2021, **179**, 106119, DOI: 10.1016/j.sab.2021.106119.

36 S. Umpierrez, T. Trejos, K. Neubauer and J. Almirall, *At. Spectrosc.*, 2006, **27**, 76–79.

37 E. Brooks, A. Mehltretter, M. Prusinowski and T. Trejos, *Forensic Chem.*, 2020, **21**, 100291, DOI: 10.1016/j.forc.2020.100291.

38 T. Trejos, R. Koons, P. Weis, S. Becker, T. Berman, C. Dalpe, M. Duecking, J. Buscaglia, T. Eckert-Lumsdon, T. Ernst, C. Hanlon, A. Heydon, K. Mooney, R. Nelson, K. Olsson, E. Schenk, C. Palenik, E. C. Pollock, D. Rudell, S. Ryland, A. Tarifa, M. Valadez, A. van Es, V. Zdanowiczq and J. Almirall, *J. Anal. At. Spectrom.*, 2013, **28**, 1270–1282, DOI: 10.1039/c3ja50128k.

39 T. Trejos, R. Koons, S. Becker, T. Berman, J. Buscaglia, M. Duecking, T. Eckert-Lumsdon, T. Ernst, C. Hanlon, A. Heydon, K. Mooney, R. Nelson, K. Olsson, C. Palenik, E. C. Pollock, D. Rudell, S. Ryland, A. Tarifa, M. Valadez, P. Weis and J. Almirall, *Anal. Bioanal. Chem.*, 2013, **405**, 5393–5409, DOI: 10.1007/s00216-013-6978-y.

40 T. Ernst, T. Berman, J. Buscaglia, T. Eckert-Lumsdon, C. Hanlon, K. Olsson, C. Palenik, S. Ryland, T. Trejos, M. Valadez and J. R. Almirall, *X-Ray Spectrom.*, 2014, **43**, 13–21, DOI: 10.1002/xrs.2437.

41 A. Akmeemana, P. Weis, R. Corzo, D. Ramos, P. Zoon, T. Trejos, T. Ernst, C. Pollock, E. Bakowska, C. Neumann and J. Almirol, *J. Chemom.*, 2021, **35**, 1–14, DOI: 10.1002/cem.3267.

42 J. Curran, T. Hicks and T. Trejos, Interpretation of Glass Evidence, *Hand Book of Trace Element Analysis*, 2020, ch. 6, DOI: 10.1002/9781119373438.ch6.

43 T. Trejos, S. Koch and A. Mehltretter, *Forensic Chem.*, 2020, **18**, 100223, DOI: 10.1016/j.forc.2020.100223.

44 R. Corzo, *et al.*, *Forensic Chem.*, 2021, **22**, 100307, DOI: 10.1016/j.forc.2021.100307.

45 T. Nakanishi, Y. Nishiwaki, N. Miyamoto, O. Shimoda, S. Watanabe, S. Muratsu, M. Takatsu, Y. Terada, Y. Suzuki, M. Kasamatsu and S. Suzuki, *Forensic Sci. Int.*, 2008, **175**, 227–234, DOI: 10.1016/j.forsciint.2007.07.001.

46 M. Bounakhla, K. Embarch, F. Zahry, E. Bilal and P. Kump, *J. Radioanal. Nucl. Chem.*, 2007, **275**, 467–478, DOI: 10.1007/s10967-005-6698-7.

47 R. Schramm, *Phys. Sci. Rev.*, 2016, **1**(9), 20160061, DOI: 10.1515/psr-2016-0061.

48 T. R. Bangia, B. A. Dhawale, V. C. Adya and M. D. Sastry, *Fresenius' J. Anal. Chem.*, 1988, **332**, 802–804, DOI: 10.1007/BF01129780.

49 S. Pathak, S. Jayabun, B. Rajeswari, N. Pathak, M. Mohapatra, A. Sengupta and R. M. Kadam, *At. Spectrosc.*, 2019, **40**(6), 215–220, DOI: 10.46770/AS.2019.06.003.

50 B. Rajeswari, S. Pathak, S. Jayabun, N. Pathak, M. Mohapatra, A. Sengupta and R. M. Kadam, *At. Spectrosc.*, 2019, **40**(6), 221–226, https://inis.iaea.org/search/search.aspx?orig_q=RN:50045768.

51 R. R. Greenberg, P. Bode and E. A. D. N. Fernandes, *Spectrochimica Acta Part B: Atom Spectrosc.*, 2011, **66**, 193–241, DOI: 10.1016/j.sab.2010.12.011.

52 ASTM E2927-16, DOI: 10.1520/E2927-16E01.

53 ASTM E2926-13, DOI: 10.1520/E2926-17.

54 V. Sharma, R. Acharya, H. K. Bagla and P. K. Pujari, *J. Anal. At. Spectrom.*, 2021, **36**, 630–643, DOI: 10.1039/D0JA00482K.

55 A. Sengupta, B. Rajeswari and R. M. Kadam, *J. Anal. At. Spectrom.*, 2020, **35**, 169–177.

56 S. Jayabun, S. Pathak and A. Sengupta, *Nucl. Instrum. Methods Phys. Res., Sect. A*, 2021, **1019**, 165854.

57 S. Jayabun, S. Pathak and A. Sengupta, *At. Spectrosc.*, 2020, **41**(4), 162–168.

58 S. K. Samanta, S. W. Raja, V. Sharma, P. S. Girkar, R. Acharya and P. K. Pujari, *J. Radioanal. Nucl. Chem.*, 2020, **325**, 923–931, DOI: 10.1007/s10967-020-07266-7.

59 N. J. G. Pearce, W. T. Perkins, J. A. Westgate, M. P. Gorton, S. E. Jackson, C. R. Neal and S. P. Chenery, *Geostand. Geoanal. Res.*, 1997, **21**, 115–141, DOI: 10.1111/j.1751-908X.1997.tb00538.x.

60 R. Acharya and P. K. Pujari, *Forensic Chem.*, 2019, **12**, 107–116, DOI: 10.1016/j.forc.2018.01.002.

61 K. B. Dasari, R. Acharya and N. L. Das, *J. Radioanal. Nucl. Chem.*, 2013, **298**, 699–705, DOI: 10.1007/s10967-013-2493-z.

62 K. B. Dasari, R. Acharya, N. L. Das and A. V. R. Reddy, *J. Radioanal. Nucl. Chem.*, 2011, **294**, 429–434, DOI: 10.1007/s10967-011-1464-5.

63 K. B. Dasari, R. Acharya and N. L. Das, *J. Radioanal. Nucl. Chem.*, 2018, **316**, 1205–1211, DOI: 10.1007/s10967-018-5863-8.

64 V. Sharma, A. Sarkar, R. Acharya, H. K. Bagla and P. K. Pujari, *Forensic Sci. Int.*, 2022, **334**, 111262.

65 M. Ferrat, D. J. Weiss, S. Strekopytov, S. Dong, H. Chen, J. Najorka, Y. Sun, S. Gupta, R. Tada and R. Sinha, *Geochim. Cosmochim. Acta*, 2011, **75**(21), 6374–6399, DOI: **10.1016/j.gca.2011.08.025**.

66 R. J. C. Brown and M. J. T. Milton, *TrAC, Trends Anal. Chem.*, 2005, **24**(3 spec. iss.), 266–274, DOI: **10.1016/j.trac.2004.11.010**.

67 M. I. Dias and M. I. Prudencio, *Microchem. J.*, 2008, **88**(2), 136–141, DOI: **10.1016/j.microc.2007.11.009**.